Hick

NACA TN 2912

NATIONAL ADVISORY COMMITTEE FOR AERONAUTICS

TECHNICAL NOTE 2912

Now Rept. 1184, 1954

THE NORMAL COMPONENT OF THE INDUCED VELOCITY IN THE VICINITY OF A LIFTING ROTOR AND SOME EXAMPLES OF ITS APPLICATION

By Walter Castles, Jr. and Jacob Henri De Leeuw

Georgia Institute of Technology

NACA

Washington
March 1953

1T

NATIONAL ADVISORY COMMITTEE FOR AERONAUTICS

TECHNICAL NOTE 2912

THE NORMAL COMPONENT OF THE INDUCED VELOCITY IN THE VICINITY OF A LIFTING ROTOR AND SOME EXAMPLES OF ITS APPLICATION

By Walter Castles, Jr. and Jacob Henri De Leeuw

SUMMARY

This paper presents a practical method for computing the approximate values of the normal component of the induced velocity at points in the flow field of a lifting rotor. Tables and graphs of the relative magnitudes of the normal component of the induced velocity are given for selected points in the longitudinal plane of symmetry of the rotor and on the lateral rotor axis.

A method is also presented for utilizing the tables and graphs to determine the interference induced velocities arising from the second rotor of a tandem- or side-by-side-rotor helicopter and the induced flow angle at a horizontal tail plane.

INTRODUCTION

This work, conducted at the Georgia Institute of Technology State Engineering Experiment Station under the sponsorship and with the financial assistance of the National Advisory Committee for Aeronautics, was undertaken in an attempt to obtain a better understanding of the induced flow in the vicinity of a lifting rotor.

Previous investigations, such as those of references 1 and 2, demonstrated that the solution of the integral for the normal component of the induced velocity at the center of the rotor could be obtained in an elementary form provided certain approximations were made as to the distribution of vorticity in the wake. However, the value of the integral for the induced-velocity component at an arbitrary point in the rotor flow field cannot, in general, be expressed in terms of elementary functions. Its numerical evaluation for a specific case presents considerable difficulty.

De Leeuw, in reference 3, investigated the feasibility of calculating the induced velocity at arbitrary points in the vicinity of the

rotor by an alternative method which consisted of (1) numerically integrating the increments induced by the vortex ring wake elements within a given distance of the point and (2) summing up the effect of the remainder of the wake by an approximate integral. This approach is quite general in that it can be applied to any wake which can be approximated by an assembly of vortex rings. It was found that the method afforded satisfactory accuracy with the expenditure of a reasonable amount of effort, since the values of the normal induced-velocity component for the isolated rings may be precomputed and tabulated for repeated use.

The scope of the present paper is limited principally to a consideration of the values of the normal component of the induced velocity at points in the longitudinal plane of symmetry and within the region likely to be occupied by the second rotor of a tandem-rotor helicopter. In addition, the values of the normal component of the induced velocity were calculated for points on the lateral axis of the tip-path plane over the distance of interest for the case of a helicopter with laterally disposed rotors.

In view of the present lack of experimental evidence as to the actual wake distribution of vorticity, the calculations for the present paper were based on the same assumptions for the wake shape as those found in references 1 and 2. These assumptions were that the wake vortex distribution consists of a straight elliptic cylinder formed by a uniform, continuous distribution of vortex rings of infinitesimal strength, lying in planes parallel to the tip-path plane and extending downstream to infinity.

SYMBOLS

a_0 constant term in Fourier series for blade flapping angle β

a_1 coefficient of cosine term of Fourier series for blade flapping angle β where

$$\beta = a_0 - a_1 \cos \psi - b_1 \sin \psi - . . .$$

b_1 coefficient of sine component of flapping angle

C_T thrust coefficient, $T/\rho\pi\Omega^2R^4$

D_f drag of fuselage

d_1	nondimensional shortest distance from a point P to a vortex ring, $\sqrt{z^2 + (x - 1)^2}$ (fig. 1)
d_2	nondimensional largest distance from a point P to a vortex ring, $\sqrt{z^2 + (x + 1)^2}$ (fig. 1)
$E(\tau)$	complete elliptic integral of first kind
$K(\tau)$	complete elliptic integral of second kind
R	radius of vortex ring; also radius of rotor
R_P	radial distance of a point P from axis of a vortex ring (fig. 1)
r	nondimensional radius vector in rotor XY-plane
T	rotor thrust
V	velocity of helicopter along flight path
V_i	normal component of velocity induced at a point P by whole wake
ΔV_i	increment of normal component of velocity induced at a point P by that portion of wake which is beyond the range of table I
v	normal component of induced velocity at center of rotor
v_r	radial component of velocity induced at a point P by a vortex ring
v_z	axial component of velocity induced at a point P by a vortex ring
W	gross weight of helicopter
w	slope of longitudinal variation of nondimensional induced velocity in plane of rotor
X,Y,Z	rotor axes (fig. 2)
x	nondimensional radial distance of a point P from axis of a vortex ring, R_P/R (fig. 1)

x', y', z' nondimensional coordinates of a point P with respect to rotor axes (fig. 3)

y slope of lateral variation of nondimensional induced velocity in plane of rotor

Z_P distance of a point P from plane of a vortex ring

z nondimensional distance of a point P from plane of a vortex ring, positive in direction of v_z, Z_P/R (fig. 1)

α angle of attack of plane of zero feathering

α_i induced angle of attack

α_f fuselage angle of attack

α_V angle of attack of tip-path plane

β_P angle between radius vector from center of rotor to a point P lying in XZ-plane and positive X-axis, positive above rotor (fig. 2)

Γ vortex strength

$\lambda = (V \sin \alpha - v)/\Omega R$

$\lambda_V = (V \sin \alpha_V - v)/\Omega R$

$\mu = V \cos \alpha/\Omega R$

$\mu_V = V \cos \alpha_V/\Omega R$

ρ density of air

$\tau = \dfrac{d_2 - d_1}{d_2 + d_1}$

ϕ_c angle between flight path and horizontal, positive below horizontal

χ angle between axis of the wake and normal to tip-path plane (fig. 2)

ψ	azimuth angle measured in XY-plane between radius vector to a point and positive X-axis, positive in going from positive X-axis to positive Y-axis
Ω	angular velocity of rotor, radians/sec

Subscripts:

B	values of back rotor of two rotors in tandem
F	values of front rotor of two rotors in tandem
v	values taken with respect to virtual axis of rotation or to tip-path plane

ANALYSIS

Velocity Induced by a Vortex Ring

It is shown in reference 4 (ch. VII, sec. 161, p. 237) that the stream function at a point P (fig. 1) in the flow field of a vortex ring of strength Γ and radius R may be expressed as

$$\psi = -\frac{\Gamma R}{2\pi}\left(d_1 + d_2\right)\left[K(\tau) - E(\tau)\right] \tag{1}$$

where R is the radius of the vortex ring, d_1R and d_2R are the least and greatest distances of the point P to the vortex ring,

$$\tau = \frac{d_2 - d_1}{d_2 + d_1} \tag{2}$$

and $K(\tau)$ and $E(\tau)$ are the complete elliptic integrals of the first and second kinds, respectively.

The flow field of a vortex ring is axially symmetric and thus the axial and radial velocity components v_z and v_r at a point P, having an axial distance Z_P from the plane of the vortex ring and a radial distance R_P from the axis of symmetry, are given by

$$v_z = -\frac{1}{R_P}\frac{d\psi}{dR_P} \tag{3}$$

and

$$v_r = \frac{1}{R_p}\frac{d\psi}{dZ_p} \tag{4}$$

It is shown in reference 3 that equations (3) and (4) may be expressed as

$$v_z = \frac{\Gamma}{2\pi xR}(AB + CDF) \tag{5}$$

and

$$v_r = \frac{-\Gamma}{2\pi xR}(AB' + CDF') \tag{6}$$

where

$$A = K(\tau) - E(\tau) \tag{7}$$

$$B = \frac{x - 1}{d_1} + \frac{x + 1}{d_2} \tag{8}$$

$$C = d_1 + d_2 \tag{9}$$

$$D = \frac{\tau E(\tau)}{1 - \tau^2} \tag{10}$$

$$F = 1 - \frac{\left(1 + x^2 + z^2\right) - d_1 d_2}{2x^2} - \frac{(1 + x)d_1{}^2 + (1 - x)d_2{}^2}{2xd_1 d_2} \tag{11}$$

$$B' = z\left(\frac{1}{d_1} + \frac{1}{d_2}\right) \tag{12}$$

$$F' = \frac{z}{x}\left(1 - \frac{1 + x^2 + z^2}{d_1 d_2}\right) \tag{13}$$

$$d_1 = \sqrt{z^2 + (x - 1)^2} \tag{14}$$

$$d_2 = \sqrt{z^2 + (x + 1)^2} \tag{15}$$

and

x nondimensional radial distance of P from axis of vortex ring, R_P/R

z nondimensional distance of P from plane of vortex ring, taken positive in direction of v_z on ring axis, Z_P/R

The values of v_z and v_r given by equations (5) and (6) become indeterminate for points on the vortex-ring axis where $x = 0$. In this case it follows from the symmetry of the flow that the radial component of induced velocity is zero, and the axial component of induced velocity is shown in reference 5 to be

$$\left(v_z\right)_{x=0} = \frac{-\Gamma}{2R}\left[\frac{1}{\left(1 + z^2\right)^{3/2}}\right] \tag{16}$$

Numerical values of v_zR/Γ, which is a nondimensional factor expressing the normal component of the induced velocity v_z in the vicinity of a vortex ring, are given in table I. The table includes a range of nondimensional axial distances of $-4.2 \leqq z \leqq 4.2$ and of nondimensional radial distances of $0 \leqq x \leqq 5.0$. The increments of z at which the values of v_zR/Γ are given are suitable for numerical integration by Simpson's rule. The tabulated values were obtained by calculation or by interpolation as indicated in the table. With the exception of those points which are close to the circumference of the vortex ring, the calculated values are accurate to four places.

Normal Component of Induced Velocity in Vicinity of a Lifting Rotor

It is assumed in this report, as in references 1 and 2, that the rotor wake vortex distribution consists of a straight elliptic cylinder formed by a uniform distribution of an infinite number of vortex rings

of infinitesimal strength, lying in planes parallel to the tip-path plane and extending downstream to infinity. The above-described vortex distribution is equivalent to a vortex sheet of uniform finite strength per unit length $d\Gamma/dZ$ measured in the Z-direction. This sheet forms a straight elliptic cylinder coinciding with the boundary of the wake.

Within the limitations of the initial assumptions, it may be shown from the results of references 1 and 2 that

$$\frac{d\Gamma}{dZ} = \frac{\Omega RC_T}{\lambda_v\left(1 - \frac{3}{2}\mu_v^2\right)} \approx \frac{\Omega RC_T}{\lambda\left(1 - \frac{3}{2}\mu^2\right)} \tag{17}$$

where the subscript v denotes values with respect to tip-path-plane coordinates.

The increment of the normal component of velocity at a point P in the vicinity of the rotor, induced by the wake vortex rings within the distance from P covered by table I, may thus be found by graphical or numerical integration. This increment constitutes about 95 percent of the total value of the normal component at the center of the rotor and a large part of the total value for most points within the region considered in this paper.

The contribution of the vortex rings beyond the range of table I to the induced velocity at P may thus be summed, with small error in the final result, by an approximate expression which is integrable.

The value of the velocity potential $\Delta\phi_P$ at P due to a closed vortex element of strength Γ is shown in reference 4 (ch. VII, sec. 150, p. 212) to be

$$\Delta\phi_P = \frac{\Gamma}{4\pi}\omega \tag{18}$$

where ω is the solid angle subtended at P by the closed vortex element.

It is a good approximation for those wake vortex rings at distances from P beyond the range of table I that the subtended solid angle at P is equal to three times that volume cut off the cone, determined by P and the ring, by a plane which is parallel to the plane of the ring and which is located a unit distance from P. It follows that

$$\Delta\phi_P \approx \frac{1}{4}\frac{d\Gamma}{dZ}\frac{zx^2R\ dz}{\left(z^2 + x^2\right)^{3/2}} \tag{19}$$

Consequently, the increment to the normal component of velocity induced at P by that portion of the wake extending from the limit of table I, at $z = z_1$, to $z = \infty$ may be obtained from the integral

$$\Delta V_i = \frac{1}{R}\frac{\partial\phi_P}{\partial z} = \frac{\partial}{\partial z}\int_{z_1}^{\infty}\frac{1}{4}\frac{d\Gamma}{dZ}\frac{zx^2\ dz}{\left(z^2 + x^2\right)^{3/2}} \tag{20}$$

It is shown in reference 3 that equation (20) may be integrated to obtain the value of ΔV_i at a point P having coordinates x', y', and z' from the center of the rotor and that the result is

$$\Delta V_i = \frac{1}{2}\frac{d\Gamma}{dZ}\left[\left(\frac{2\sqrt{c}}{q} - \frac{2cz_2 + b}{q\sqrt{K}}\right)\left(1 - \frac{4ac + b^2}{cq}\right) + \frac{\left(b^2 - 2ac\right)z_2 + ab}{cqK^{3/2}}\right] \tag{21}$$

where

$$a = (x' - z' \tan \chi)^2 + (y')^2 \tag{22}$$

$$b = -2x' \tan \chi \tag{23}$$

$$c = 1 + \tan^2\chi \tag{24}$$

$$q = 4ac - b^2 \tag{25}$$

$$K = a + bz_2 + cz_2{}^2 \tag{26}$$

and

$$z_2 = z_1 - z' \tag{27}$$

For the point P(0,0,0) the value of ΔV_i given by equation (21) becomes indeterminate. It is possible, however, to substitute the zero coordinates in the equation before integrating. Doing so yields

$$\left(\Delta V_i\right)_{0,0,0} = -\frac{1}{8z_1^{\,2}}\frac{d\Gamma}{dZ}\cos^3\chi\left(3\cos^2\chi - 1\right) \tag{28}$$

The normal component of the induced velocity at any point P(x',y',z') may thus be found in terms of $d\Gamma/dZ$ by adding the increment obtained from the numerical integration of the values induced by the wake vortex rings within the range covered by table I to ΔV_i, obtained from equation (21) or (28).

In the present analysis where the rotor wake vortex distribution is approximated by a straight elliptic cylinder there arises the question as to whether the wake angle should be taken as that at the rotor or that in the ultimate wake. As the induced velocity distributions in the vicinity of the rotor are more sensitive to changes in position of the adjacent vortex elements than to changes in position of the vortex elements at the greater distances, the wake angle at the rotor will be used in the present analysis.

It follows from figure 2 that, for $\chi < 90^\circ$, or $\lambda_v = \lambda \cos a_1 + \mu \sin a_1 < 0$,

$$\chi = \tan^{-1}\left(\frac{-\mu_v}{\lambda_v}\right) = \tan^{-1}\left(\frac{-\mu}{\lambda}\right) + a_1 \tag{29}$$

and, for $\chi > 90^\circ$, or $\lambda_v = \lambda \cos a_1 + \mu \sin a_1 > 0$,

$$\chi = \cot^{-1}\left(\frac{-\mu_v}{\lambda_v}\right) = \cot^{-1}\left(\frac{-\mu}{\lambda}\right) - a_1 \tag{30}$$

In the above equations a_1 is the coefficient of the cosine term of the Fourier series for the blade flapping angle

$$\beta = a_0 - a_1 \cos \psi - b_1 \sin \psi - \ldots$$

where β is measured from the plane of zero feathering.

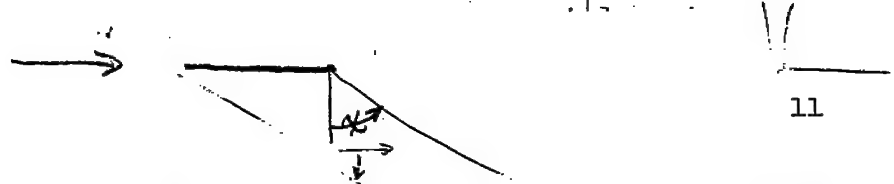

For $\chi = 90^{\circ}$, equation (21) is indeterminant. However, by replacing $d\Gamma/dz$ in equation (20) by its equivalent $\left(\frac{d\Gamma}{dx}\right) \tan \chi$ after performing the indicated differentiation with respect to z, it can be shown that for this wake angle

$$\Delta V_i = \frac{1}{4}\frac{d\Gamma}{dx}\left\{\frac{1}{(z')^2} - \frac{x_1}{(z')^2\left[(z')^2 + x_1^{\,2}\right]^{1/2}} - \frac{x_1}{(z')^2\left[(z')^2 + x_1^{\,2}\right]^{3/2}}\right\} \tag{31}$$

where the integral now covers the region from $x = x_1$ to $x = \infty$ and

$$\frac{d\Gamma}{dx} = -\frac{\Omega R C_T}{\mu_v\left(1 - \frac{3}{2}\mu_v^{\,2}\right)} \approx -\frac{\Omega R C_T}{\mu\left(1 - \frac{3}{2}\mu^2\right)}$$

$\lambda \Omega R = V \sin\alpha - v$

RESULTS

The results are presented in the form of tables and graphs of the ratio of the normal component of the induced velocity V_i at any point $P\left(\beta_P, X/R \text{ or } \beta_P, Y/R\right)$, as in figure 2, to the normal component of the induced velocity v at the center of the rotor. It is shown in reference 2 that

$$v \approx \frac{\frac{1}{2}\Omega R C_T}{\left(1 - \frac{3}{2}\mu_v^{\,2}\right)\sqrt{\lambda_v^{\,2} + \mu_v^{\,2}}} \approx \frac{\frac{1}{2}\Omega R C_T}{\left(1 - \mu^2\right)\sqrt{\lambda^2 + \mu^2}} \tag{32}$$

Consequently, the value of V_i at P may be easily computed from the values of V_i/v in the tables and graphs.

Table II gives the values of V_i/v for $-3.2 \leqq X/R \leqq 3.2$ and $\tan \beta_P = -1/2, -1/4, 0, 1/4,$ and $1/2$. Table III gives the values of V_i/v along the lateral axis of the tip-path plane. Figures 4(a) to 4(i) show the lines of constant values of V_i/v in the longitudinal plane of symmetry for wake angles having tangents of 0, 1/4, 1/2, 1, 2, 4, ∞, -4,

and -2. Figures 5 and 6 show the variation of V_i/v with X for points on the longitudinal and lateral axes of the tip-path plane.

APPLICATION OF RESULTS

Determination of Mean Value of Normal Component of Induced Velocity Over Front and Back Rotors of a Tandem-Rotor Helicopter

Making the approximation that the mean values of the induced velocity are the values at the centers of the respective rotors, and being given the flight-path velocity, climb angle, gross weight, fuselage drag, fuselage angle of attack, thrust and tip speed of the front and rear rotors, and the geometry of the helicopter, the mean values of the induced velocities may be found as follows:

The angles of attack α_v of the tip-path planes of the front and rear rotors are very nearly

$$\alpha_v = \phi_c - \frac{D_f \cos \phi_c}{W - D_f \sin \phi_c} \tag{33}$$

where

ϕ_c angle between flight path and horizontal, positive below horizontal

D_f drag of fuselage

W gross weight

Denote values of the parameters of the front rotor by the subscript F and of the back rotor by the subscript B. Then

$$\mu_{v_F} = \left(\frac{V}{\Omega R}\right)_F \cos \alpha_v \tag{34}$$

and

$$\mu_{v_B} = \left(\frac{V}{\Omega R}\right)_B \cos \alpha_v \tag{35}$$

As a first approximation, the interference induced velocity at the front rotor due to the thrust of the back rotor may be neglected. Then

$$\lambda_{v_F} = \left(\frac{V}{\Omega R}\right)_F \sin \alpha_v - \frac{v_F}{(\Omega R)_F} \tag{36}$$

where the value of v_F is given by equation (32) or, for $\mu_{v_F} > 0.15$,

$$\frac{v}{\Omega R} \approx \frac{\frac{1}{2} C_T}{\mu_v\left(1 - \frac{3}{2} \mu_v{}^2\right)} \tag{37}$$

The value of X_F may then be obtained from equation (29) or (30). When X, α_v, α_f, v_F, and the geometry of the helicopter are known, the position of the center of the rear rotor with respect to the front rotor can be determined. Then the nondimensional velocity V_i/v induced at the center of the rear rotor, because of the thrust of the front rotor, may be obtained by interpolation from one of figures 4(a) to 4(i) for the appropriate value of X_F. The approximate value of $v_{B_{total}}$ is then

$$v_{B_{total}} = \left(V_i/v\right) v_F + v_B \tag{38}$$

where v_B can be obtained from equation (32) or (37). The approximate values of λ_{v_B}, X_B, and, thus, the interference induced velocity at the front rotor may be found to evaluate $v_{F_{total}}$. In general, it will be necessary to iterate $v_{B_{total}}$ for an accurate result, because of the rapid variation of the interference induced velocity at the rear rotor with change in the wake angle of the front rotor and with position of the rear rotor with respect to the tip-path plane of the front rotor.

For a tandem-rotor helicopter, having approximately equally loaded rotors of equal size spaced approximately 1 rotor diameter apart with small vertical offset and operating in the high-speed flight range, it is seen from figures 4(f) and 4(g) that

$$\frac{v_{F_{total}}}{\Omega R} \approx \frac{0.47C_T}{\mu_v\left(1 - \frac{3}{2}\mu_v^2\right)} \tag{39}$$

and

$$\frac{v_{B_{total}}}{\Omega R} \approx \frac{1.25C_T}{\mu_v\left(1 - \frac{3}{2}\mu_v^2\right)} \tag{40}$$

Determination of Longitudinal Variation of Normal Component of Induced Velocity Over Front and Back Rotors of a Tandem-Rotor Helicopter

If the normal component V_i of the induced velocity at $P(r,\psi)$ on the rotor disk is approximated by the expression

$$\frac{V_i}{\Omega R} = -\frac{v}{\Omega R} + yr \sin\psi + wr \cos\psi \tag{41}$$

it may be shown from the results given in reference 2 that, for a single rotor,

$$w \approx -\frac{4}{3}\left[\left(1 - 1.8\mu_v^2\right)\sqrt{1 + \left(\frac{\lambda_v}{\mu_v}\right)^2} - \sqrt{\left(\frac{\lambda_v}{\mu_v}\right)^2}\right]\frac{v}{\Omega R} \tag{42}$$

The increments in w arising from the second rotor of a tandem-rotor helicopter, to be added to the values given by equation (42) for the front and rear rotors, may be obtained in the general case from the values of V_i/v from the figures at $r = 0.75$ and $\psi = 0$ and π on the respective rotors. Thus,

$$\Delta w = -\left[\left(\frac{V_i}{v}\right)_{\substack{\psi=0\\ r=0.75}} - \left(\frac{V_i}{v}\right)_{\substack{\psi=\pi\\ r=0.75}}\right]\frac{2}{3}\frac{v}{\Omega R} \tag{43}$$

For high-speed flight and small overlaps between the rotor disks

$$\Delta w_F \approx \frac{1}{6}\frac{v_B}{\Omega R} \tag{44}$$

and, with less accuracy,

$$\Delta w_B \approx \frac{1}{4}\frac{v_F}{\Omega R} \tag{45}$$

Determination of Induced Flow Angle at a Horizontal Tail Plane

When the values of α_v, $v/\Omega R$, χ, and α_f for the rotor or rotors in question have been determined and when the helicopter flight condition under consideration is known, the geometric position, and thus the values of Z/R and X/R, of the horizontal tail plane may be calculated and the value or values of V_i/v, found from the figures. Then the induced angle $\alpha_{i_{tail}}$ at the tail plane is approximately

$$\alpha_{i_{tail}} \approx -\frac{\left(\frac{V_i}{v}\,v\right)_F + \left(\frac{V_i}{v}\,v\right)_B}{V\cos\alpha_f} \tag{46}$$

CONCLUDING DISCUSSION

The assumption that the planes of the wake vortex rings remain parallel to the tip-path plane is the only one of the various initial assumptions as to the wake distribution of vorticity which appears likely to affect the engineering accuracy of these results at the higher flight speeds. It is the opinion of the senior author that the present investigation and that of reference 1 indicate that the planes of the wake vortex rings must be tilted to the rear as they leave the rotor, possibly approaching a tilt angle in the ultimate wake of half the wake angle χ. The quantitative effects of such a tilting of the wake vortex rings may not be large, as the increments of the radial components of the induced velocity introduced because of the tilt of the wake vortex rings will tend to compensate for the decrease in the normal component.

For the lower-speed flight conditions the initial assumptions as to the wake distribution of vorticity are compatible only with the assumption that the generating rotor is lightly loaded and has blades with constant circulation along the radii. Caution should therefore be exercised in applying the results of this analysis to points on or close to the disk of a specific rotor which is operating at the lower flight-path velocities.

At the center of the rotor, where the values of the induced velocity calculated by the method presented in this report could be compared with the values obtained from the exact integral, the error was in every case less than 1 percent. However, for those points in the flow field that lie close to the wake vortex sheet, there are irregularities in the tabulated values of V_i/v caused by difficulties with the interpolations in the table of the values of the normal component of the induced velocity for the vortex rings.

It should be noted that the present analysis neglects the effects of the lateral dissymmetry of the blade-bound vortices and the consequent lateral dissymmetry of the wake vortex elements which occur in forward flight. Numerical calculations show that the effects of these lateral dissymmetries on the induced velocity distributions are small at points of interest outside the boundaries of the rotor disk or wake but should be taken into account in computing the longitudinal and lateral distributions across the rotor disk. The first-order effects of the lateral variation in the strength of the blade-bound vortices are accounted for by equation (42) and the first-order effects of the lateral variation in the strength of the wake vortices may be taken into account by use of a value of

$$y \approx 2\mu_V \frac{v}{\Omega R} \approx 2\mu \frac{v}{\Omega R}$$

in equation (41).

In order to construct figures 4 to 6 it was necessary to compute a large number of values of V_i/v in addition to those listed in table II. However, as these additional points were at scattered locations, and consequently of little use for any other purpose, they have been omitted from this report.

Since the wake angles of the rotors of helicopters operating in the upper half of their speed range fall in a narrow band between 80° and 85°, it would be useful to have the induced velocity distribution for a wake angle of, say, 82°. However, investigation showed that in order to obtain sufficiently accurate values for this wake angle it would first

be necessary to compute a large number of additional values of the induced velocity of the vortex ring for the region within two-tenths of a ring radius from the periphery of the ring. The computations for the 82° wake angle were therefore too lengthy for the results to be included in the present report.

It appears from the results of this investigation that the interference induced velocity at the rear rotor of a tandem-rotor helicopter in high-speed flight, due to the thrust of the front rotor, is of the same order of magnitude and of the same sign as the self-induced velocity. Consequently, the interference induced velocity should be taken into account in longitudinal stability calculations and in computing the equilibrium values of the mean blade angle and torque coefficients. The interference induced velocity at the front rotor of a tandem-rotor helicopter in high-speed flight is of the order of 7 percent of the self-induced velocity and is opposite in sign.

The longitudinal gradient of the interference induced velocities at both rotors of a tandem-rotor helicopter in high-speed flight is of opposite sign to the longitudinal gradients of the self-induced velocities, and, consequently, will have the effect of reducing the required equilibrium values of b_1, the coefficient of the sine component of the flapping angle.

For side-by-side-rotor helicopters in high-speed flight the mean values of the interference induced velocities are of the order of 15 percent of the self-induced velocities and are opposite in sign. The lateral gradients of the mutual interference induced velocities are large for the adjacent portions of the rotors. These large gradients may cause early tip stall if the rotor rotation is such that the retreating blades are in this adjacent rotor position.

The normal component of the induced velocity inside the wake of a helicopter rotor in high-speed flight appears to reach its maximum and final value of about twice the value at the center of the rotor at a distance of about 1 rotor radius downstream from the center of the rotor. For hovering and the lower forward speeds the induced velocity inside the wake reaches its final value of about twice that at the center of the rotor at a distance of about 2 rotor radii downstream.

Georgia Institute of Technology
Atlanta, Ga., August 11, 1952

REFERENCES

1. Coleman, Robert P., Feingold, Arnold M., and Stempin, Carl W.: Evaluation of the Induced-Velocity Field of an Idealized Helicopter Rotor. NACA ARR L5E10, 1945.

2. Drees, Meijer, Jr.: A Theory of Airflow Through Rotors and Its Application to Some Helicopter Problems. The Jour. Helicopter Assoc. (Great Britain), vol. 3, no. 2, July-Aug.-Sept. 1949, pp. 79-104.

3. De Leeuw, Jacob Henri: The Normal Component of the Induced Velocity Near a Vortex Ring and Its Application to Lifting Rotor Problems. Master's Thesis, Daniel Guggenheim School of Aero., Ga. Inst. of Tech., Dec. 1951.

4. Lamb, Horace: Hydrodynamics. Sixth ed., Dover Publications, 1945.

5. Glauert, H.: On the Contraction of the Slipstream of an Airscrew. R. & M. No. 1067, British A.R.C., 1926.

TABLE I

NONDIMENSIONAL VALUES OF NORMAL COMPONENT

OF INDUCED VELOCITY IN VICINITY OF A VORTEX RING

$\left[x = R_p/R; \ z = \pm Z_p/R\right]$

z	$v_z R/\Gamma$													
	x = 0 (a)	x = 0.1 (a)	x = 0.2 (a)	x = 0.3 (a)	x = 0.4 (a)	x = 0.5 (a)	x = 0.6 (a)	x = 0.7 (a)	x = 0.8 (a)	x = 0.9 (a)	x = 1.0 (a)	x = 1.1 (a)	x = 1.2 (a)	x = 1.3 (a)
0	0.5000	0.5038	0.5156	0.5369	0.5707	0.6228	0.7053	0.8461	1.1293	1.9630	-------	-1.2627	-0.5324	-0.3062
.1	.4926	.4961	.5070	.5264	.5569	.6025	.6711	.7768	.9397	1.0938	0.2687	-.5298	-.3961	-.2633
.2	.4714	.4742	.4827	.4974	.5193	.5494	.5881	.6304	.6496	.5501	.2126	-.1094	-.1941	-.1756
.4	.4002	.4010	.4032	.4064	.4093	.4098	.4034	.3825	.3365	.2568	.1550	.0674	-.0096	-.0438
.6	.3153	.3147	.3128	.3089	.3022	.2911	.2735	.2476	.2121	.1682	.1201	.0747	.0371	.0099
.8	.2381	.2370	.2338	.2281	.2196	.2076	.1919	.1721	.1486	.1225	.0956	.0698	.0470	.0284
1.0	.1768	.1758	.1728	.1677	.1604	.1508	.1391	.1253	.1099	.0934	.0768	.0607	.0460	.0332
1.3	.1133	.1127	.1106	.1073	.1027	.0969	.0900	.0822	.0738	.0649	.0560	.0473	.0391	.0316
1.6	.0744	.0740	.0728	.0708	.0681	.0647	.0608	.0663	.0516	.0465	.0415	.0364	.0315	.0269
2.1	.0397	.0396	.0391	.0382	.0371	.0357	.0341	.0322	.0302	.0281	.0259	.0236	.0209	.0192
2.6	.0231	.0231	.0228	.0225	.0220	.0213	.0206	.0197	.0188	.0178	.0168	.0156	.0146	.0135
3.4	.0112	.0112	.0111	.0110	.0109	.0106	.0104	.0101	.0098	.0095	.0091	.0087	.0083	.0079
4.2	.0062	.0062	.0062	.0061	.0061	.0060	.0059	.0058	.0056	.0055	.0054	.0052	.0050	.0048

z	$v_z R/\Gamma$													
	x = 1.4 (a)	x = 1.5 (a)	x = 1.6 (a)	x = 1.7 (a)	x = 1.8 (a)	x = 1.9 (a)	x = 2.0 (a)	x = 2.1 (b)	x = 2.2 (b)	x = 2.3 (b)	x = 2.4 (b)	x = 2.5 (b)	x = 2.6 (a)	x = 2.7 (b)
0	-0.2010	-0.1424	-0.1060	-0.0817	-0.0647	-0.0524	-0.0431	-0.0358	-0.0300	-0.0254	-0.0219	-0.0191	-0.0170	-0.0151
.1	-.1833	-.1336	-.1011	-.0788	-.0629	-.0511	-.0423	-.0350	-.0292	-.0250	-.0216	-.0189	-.0169	-.0150
.2	-.1411	-.1112	-.0882	-.0709	-.0577	-.0477	-.0398	-.0334	-.0283	-.0241	-.0209	-.0183	-.0164	-.0146
.4	-.0559	-.0667	-.0527	-.0471	-.0414	-.0362	-.0315	-.0272	-.0238	-.0208	-.0183	-.0164	-.0147	-.0132
.6	-.0076	-.0175	-.0218	-.0241	-.0241	-.0230	-.0215	-.0199	-.0181	-.0163	-.0149	-.0136	-.0123	-.0112
.8	.0141	.0038	-.0031	-.0076	-.0103	-.0117	-.0122	-.0121	-.0119	-.0115	-.0108	-.0101	-.0095	-.0089
1.0	.0226	.0141	.0073	.0026	-.0009	-.0034	-.0060	-.0066	-.0059	-.0062	-.0067	-.0068	-.0067	-.0066
1.3	.0249	.0190	.0141	.0100	.0067	.0040	.0020	.0008	-.0006	-.0016	-.0022	-.0029	-.0032	-.0034
1.6	.0226	.0187	.0153	.0122	.0096	.0074	.0060	.0045	.0031	.0021	.0012	.0002	-.0005	-.0009
2.1	.0171	.0151	.0132	.0115	.0099	.0085	.0072	.0062	.0052	.0043	.0035	.0028	.0020	.0015
2.6	.0124	.0113	.0103	.0093	.0084	.0075	.0067	.0059	.0052	.0046	.0040	.0034	.0029	.0025
3.4	.0075	.0070	.0066	.0062	.0058	.0054	.0050	.0046	.0042	.0039	.0036	.0033	.0030	.0027
4.2	.0047	.0045	.0043	.0041	.0039	.0037	.0035	.0033	.0031	.0029	.0027	.0025	.0024	.0023

[a]Values obtained by calculation.

[b]Values obtained by interpolation.

TABLE I.- Concluded

NONDIMENSIONAL VALUES OF NORMAL COMPONENT

OF INDUCED VELOCITY IN VICINITY OF A VORTEX RING - Concluded

z	v_zR/Γ											
	x = 2.8 (b)	x = 2.9 (b)	x = 3.0 (b)	x = 3.1 (b)	x = 3.2 (a)	x = 3.3 (b)	x = 3.4 (b)	x = 3.5 (b)	x = 3.6 (b)	x = 3.7 (b)	x = 3.8 (b)	x = 3.9 (b)
0	-0.0135	-0.0121	-0.0109	-0.0097	-0.0086	-0.0077	-0.0070	-0.0064	-0.0058	-0.0053	-0.0049	-0.0045
.1	-.0133	-.0120	-.0108	-.0096	-.0085	-.0076	-.0069	-.0063	-.0058	-.0053	-.0049	-.0045
.2	-.0129	-.0117	-.0105	-.0095	-.0084	-.0075	-.0068	-.0062	-.0057	-.0052	-.0048	-.0044
.4	-.0119	-.0107	-.0098	-.0089	-.0079	-.0072	-.0065	-.0060	-.0055	-.0051	-.0047	-.0043
.6	-.0102	-.0094	-.0087	-.0079	-.0071	-.0065	-.0059	-.0054	-.0050	-.0046	-.0043	-.0040
.8	-.0082	-.0076	-.0070	-.0065	-.0061	-.0056	-.0051	-.0047	-.0044	-.0041	-.0039	-.0036
1.0	-.0063	-.0061	-.0058	-.0054	-.0050	-.0047	-.0044	-.0041	-.0038	-.0036	-.0034	-.0032
1.3	-.0036	-.0038	-.0037	-.0036	-.0034	-.0032	-.0031	-.0029	-.0028	-.0027	-.0026	-.0025
1.6	-.0012	-.0016	-.0017	-.0018	-.0019	-.0019	-.0019	-.0020	-.0019	-.0019	-.0019	-.0018
2.1	.0011	.0007	.0004	.0001	-.0001	-.0003	-.0004	-.0005	-.0006	-.0007	-.0008	-.0008
2.6	.0022	.0019	.0016	.0013	.0010	.0008	.0007	.0005	.0003	.0002	.0001	0
3.4	.0024	.0021	.0019	.0017	.0016	.0014	.0013	.0011	.0010	.0009	.0007	.0006
4.2	.0022	.0021	.0020	.0019	.0019	.0017	.0016	.0015	.0014	.0012	.0011	.0010

z	v_zR/Γ											
	x = 4.0 (a)	x = 4.1 (b)	x = 4.2 (b)	x = 4.3 (b)	x = 4.4 (b)	x = 4.5 (b)	x = 4.6 (b)	x = 4.7 (b)	x = 4.8 (b)	x = 4.9 (b)	x = 5.0 (a)	
0	-0.0042	-0.0039	-0.0037	-0.0034	-0.0032	-0.0030	-0.0028	-0.0026	-0.0024	-0.0022	-0.0021	
.1	-.0042	-.0039	-.0037	-.0034	-.0032	-.0030	-.0028	-.0026	-.0024	-.0022	-.0021	
.2	-.0041	-.0038	-.0036	-.0033	-.0031	-.0029	-.0027	-.0025	-.0024	-.0022	-.0021	
.4	-.0040	-.0037	-.0035	-.0032	-.0030	-.0028	-.0026	-.0024	-.0023	-.0021	-.0020	
.6	-.0037	-.0035	-.0033	-.0030	-.0029	-.0027	-.0025	-.0023	-.0022	-.0021	-.0020	
.8	-.0034	-.0032	-.0030	-.0028	-.0026	-.0025	-.0023	-.0022	-.0020	-.0019	-.0018	
1.0	-.0030	-.0028	-.0026	-.0025	-.0023	-.0022	-.0021	-.0020	-.0019	-.0018	-.0017	
1.3	-.0024	-.0022	-.0021	-.0020	-.0020	-.0019	-.0018	-.0017	-.0017	-.0016	-.0015	
1.6	-.0018	-.0017	-.0017	-.0016	-.0015	-.0015	-.0015	-.0014	-.0014	-.0013	-.0013	
2.1	-.0009	-.0009	-.0009	-.0009	-.0009	-.0009	-.0009	-.0009	-.0009	-.0009	-.0008	
2.6	-.0001	-.0002	-.0003	-.0004	-.0004	-.0005	-.0005	-.0005	-.0005	-.0005	-.0005	
3.4	.0005	.0004	.0003	.0002	.0002	.0001	.0001	0	0	0	0	
4.2	.0009	.0008	.0007	.0006	.0005	.0005	.0004	.0004	.0003	.0003	.0002	

[a]Values obtained by calculation.

[b]Values obtained by interpolation.

TABLE II

NONDIMENSIONAL VALUES OF NORMAL COMPONENT OF INDUCED VELOCITY IN LONGITUDINAL PLANE OF SYMMETRY OF A LIFTING ROTOR FOR $\chi \leqq 90^\circ$

[For flight conditions for which $\chi > 90^\circ$ and a developed wake exists, values of V_i/v for $(\chi, X/R, \beta_P)$ are the same as those for $(180^\circ - \chi, X/R, -\beta_P)$]

X/R	V_i/v for values of $\tan \beta_P$ of -				
	-1/2	-1/4	0	1/4	1/2
			$\chi = 0^\circ$ (a)		
0	1.000	1.000	1.000	1.000	1.000
.40	1.220	1.112	1.000	.888	.780
.80	1.555	1.368	1.000	.632	.445
.90	1.643	1.495	1.000	.505	.357
1.00	-----	-----	.500	.363	.282
1.10	-.224	-.253	0	.253	.224
1.20	-.180	-.180	0	.180	.180
1.60	-.088	-.067	0	.067	.088
2.00	-.053	-.038	0	.038	.053
3.20	-.019	-.012	0	.012	.019

X/R	V_i/v for values of $\tan \beta_P$ of -				
	-1/2	-1/4	0	1/4	1/2
			$\chi = 14.04^\circ$ ($\tan \chi = 1/4$) (b)		
-3.20	0.011	0.001	-0.010	-0.020	-0.023
-2.00	.028	.012	-.027	-.061	-.063
-1.60	.057	.026	-.046	-.101	-.105
-1.20	.132	.099	-.108	-.232	-.200
-.80	.363	.521	.860	1.245	1.406
-.40	.729	.835	.948	1.059	1.170
0	1.000	1.000	1.000	1.000	1.000
.40	1.262	1.161	1.052	.940	.828
.80	1.626	1.479	1.139	.746	.526
1.20	-----	-.036	.150	.281	.242
1.40	-.042	-----	------	------	------
1.60	-----	.004	.079	.121	.126
2.00	-.013	.007	.046	.073	.077
3.20	-.001	.004	.016	.034	.028

[a]Value of V_i/v changes 2.000 units in passing through boundary of wake. Values are axially symmetric about rotor axis and antisymmetric about tip-path plane; values about which they are antisymmetric are 1.000 for $X/R < 1$ and 0 for $X/R > 1$.

[b]Value of V_i/v changes 1.940 units in passing through boundary of wake.

NACA

TABLE II.- Continued

NONDIMENSIONAL VALUES OF NORMAL COMPONENT OF INDUCED VELOCITY IN LONGITUDINAL PLANE OF SYMMETRY OF A LIFTING ROTOR FOR $\chi \leq 90^\circ$ - Continued

X/R	V_i/v for values of $\tan \beta_p$ of -				
	-1/2	-1/4	0	1/4	1/2
	$\chi = 26.56^\circ$ ($\tan \chi = 1/2$) (c)				
-3.20	0.005	-0.004	-0.016	-0.024	-0.026
-2.00	.019	-.006	-.044	-.067	-.065
-1.60	.034	-.016	-.073	-.120	-.109
-1.20	.089	.038	-.180	-.261	-.198
-.80	.305	.426	.738	------	------
-.40	.687	.788	.899	1.046	1.126
0	1.000	1.000	1.000	1.000	1.000
.40	1.314	1.211	1.101	.987	.874
.80	1.692	1.582	1.261	.860	.604
1.20	1.803	------	.328	.403	.305
1.60	.113	.125	.167	.191	.166
2.00	.088	.084	.105	.115	.105
3.20	.038	.037	.041	.044	.040

X/R	V_i/v for values of $\tan \beta_p$ of -				
	-1/2	-1/4	0	1/4	1/2
	$\chi = 45.00^\circ$ ($\tan \chi = 1$) (d)				
-3.20	-0.002	-0.010	-0.019	-0.025	-0.023
-2.00	-.001	-.028	-.060	-.071	-.060
-1.60	.006	-.039	-.107	-.122	-.096
-1.20	.036	-.039	-.265	-.249	-.172
-.80	.217	.285	.535	------	-.142
-.40	.622	.719	.824	.927	1.046
0	1.000	1.000	1.000	1.000	1.000
.40	1.381	1.283	1.176	1.062	.947
.80	1.782	1.711	1.465	1.048	.740
1.20	1.957	1.866	.683	.593	.423
1.60	1.829	.467	.410	.332	.247
2.00	------	.372	.272	.215	.164
3.20	.307	.165	.113	.087	.066

X/R	V_i/v for values of $\tan \beta_p$ of -				
	-1/2	-1/4	0	1/4	1/2
	$\chi = 63.43^\circ$ ($\tan \chi = 2$) (e)				
-3.20	-0.008	-0.021	-0.022	-0.020	-0.020
-2.00	-.015	-.043	-.064	-.069	-.051
-1.60	-.020	-.067	-.119	-.116	-.083
-1.20	-.012	-.105	-.294	-.238	-.140
-.80	.124	.140	.326	-.320	-.144
-.40	.550	.639	.746	.858	------
0	1.000	1.000	1.000	1.000	1.000
.40	1.460	1.366	1.254	1.144	1.032
.80	1.886	1.849	1.674	1.265	.911
1.20	2.022	2.098	1.240	.900	.600
1.60	2.030	2.098	.878	.582	.384
2.00	2.026	------	.653	.401	.262
3.20	2.017	.776	.278	.181	.100

[c]Value of V_i/v changes 1.789 units in passing through boundary of wake.

[d]Value of V_i/v changes 1.414 units in passing through boundary of wake.

[e]Value of V_i/v changes 0.894 units in passing through boundary of wake.

TABLE II.- Concluded

NONDIMENSIONAL VALUES OF NORMAL COMPONENT OF INDUCED VELOCITY IN LONGITUDINAL PLANE OF SYMMETRY OF A LIFTING ROTOR FOR $\chi \leqq 90^{\circ}$ - Concluded

X/R	V_i/v for values of $\tan \beta_p$ of -				
	-1/2	-1/4	0	1/4	1/2
	$\chi = 75.97^{\circ}$ ($\tan \chi = 4$) (f)				
-3.20	-0.011	-0.019	-0.026	-0.022	-0.014
-2.00	-.025	-.052	-.072	-.065	-.043
-1.60	-.035	-.084	-.124	-.101	-.067
-1.20	-.043	-.136	-.309	-.213	-.110
-.80	.062	.054	.166	-.193	-.087
-.40	.485	.549	.675	------	.483
0	1.000	1.000	1.000	1.000	1.000
.40	1.494	1.427	1.325	1.165	1.096
.80	1.576	1.942	1.834	1.436	1.053
1.20	1.895	2.150	------	1.183	.763
1.60	1.250	2.086	1.384	.869	.530
2.00	.967	2.063	1.187	.623	.377
3.20	.735	2.022	.785	.328	.169

X/R	V_i/v for values of $\tan \beta_p$ of -				
	-1/2	-1/4	0	1/4	1/2
	$\chi = 90.00^{\circ}$ (g)				
-3.20	-0.016	-0.022	-0.026	-0.022	-0.016
-2.00	-.035	-.060	-.078	-.060	-.035
-1.60	-.052	-.097	-.137	-.097	-.052
-1.20	-.076	-.182	-.331	-.182	-.076
-1.00	------	------	-.621	------	------
-.80	-.010	-.057	-.075	-.057	-.010
-.40	.414	.519	.564	.519	.414
0	1.000	1.000	1.000	1.000	1.000
.40	1.193	1.312	1.436	1.312	1.193
.80	1.266	1.664	2.075	1.664	1.266
1.20	1.046	1.602	2.331	1.602	1.046
1.60	.804	1.354	2.137	1.354	.804
2.00	.619	1.175	2.078	1.175	.619
3.20	.318	.774	2.026	.774	.318

[f]Value of V_i/v changes 0.485 units in passing through boundary of wake.

[g]Values of V_i/v are symmetric about tip-path plane; for $\beta_p = 0$ they are antisymmetric about the value 1 at $X = 0$. Values for $\beta_p = 0$ obtained by extrapolation.

NACA

TABLE III

NONDIMENSIONAL VALUES OF NORMAL COMPONENT OF

INDUCED VELOCITY ON LATERAL AXIS OF A LIFTING ROTOR

$\pm Y/R$	V_i/v for values of $\tan X$ of -				
	0	1	2	4	∞
0	1.000	1.000	1.000	1.000	1.000
.40	1.000	1.000	1.000	1.000	1.000
.60	1.000	-----	-----	------	.978
.80	1.000	-----	-----	------	.904
1.10	0	-----	-.702	-1.071	-1.399
1.20	0	-.235	-.548	-.693	-.809
1.40	0	-.158	-.319	-.401	-.428
1.60	0	-.114	-.239	-.256	-.281
2.00	0	-.068	-.119	-.144	-.154
3.20	0	-.026	-.041	-.049	-.053

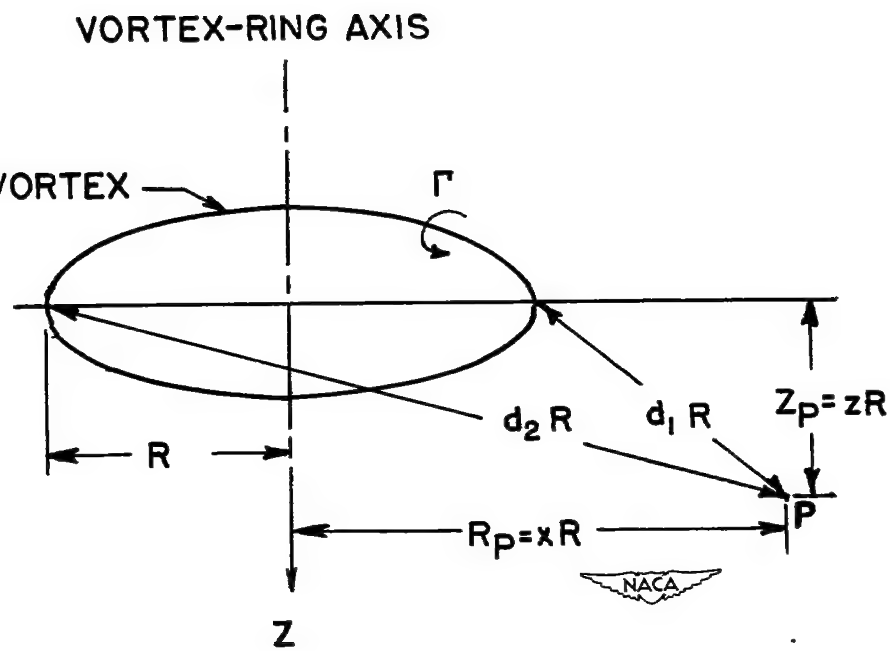

Figure 1.- Coordinates for vortex ring and table I.

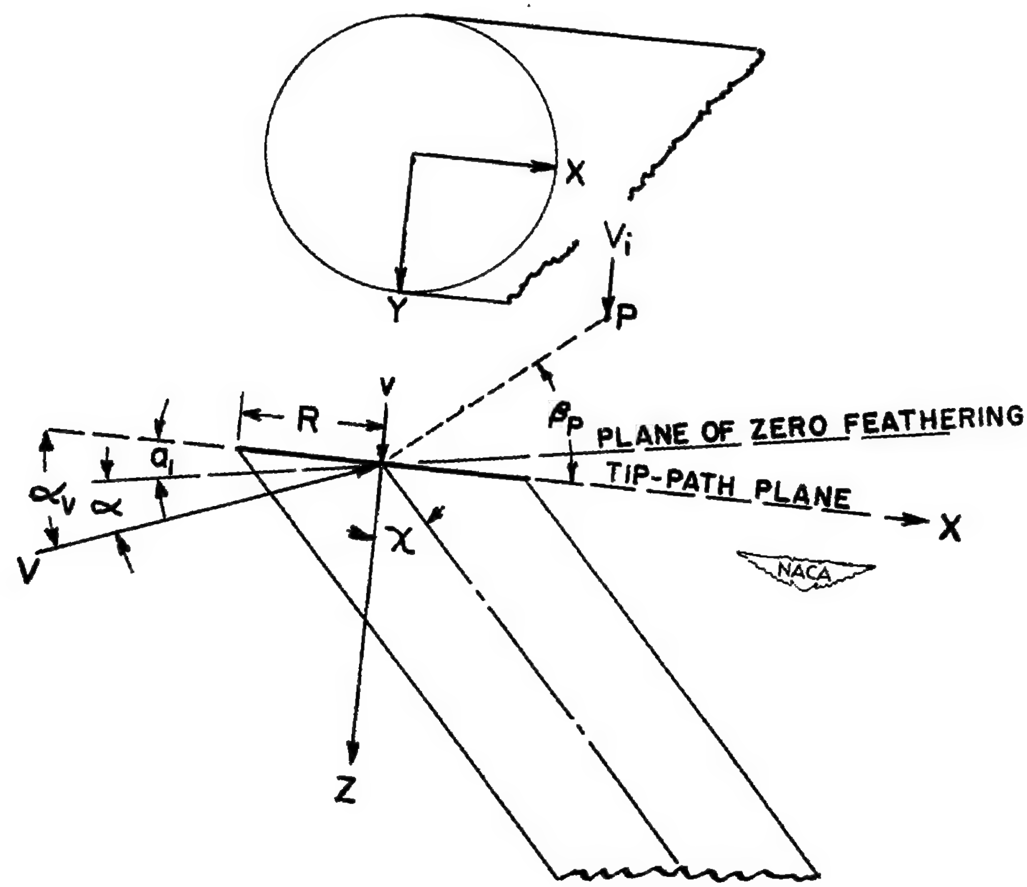

Figure 2.- Geometry of wake.

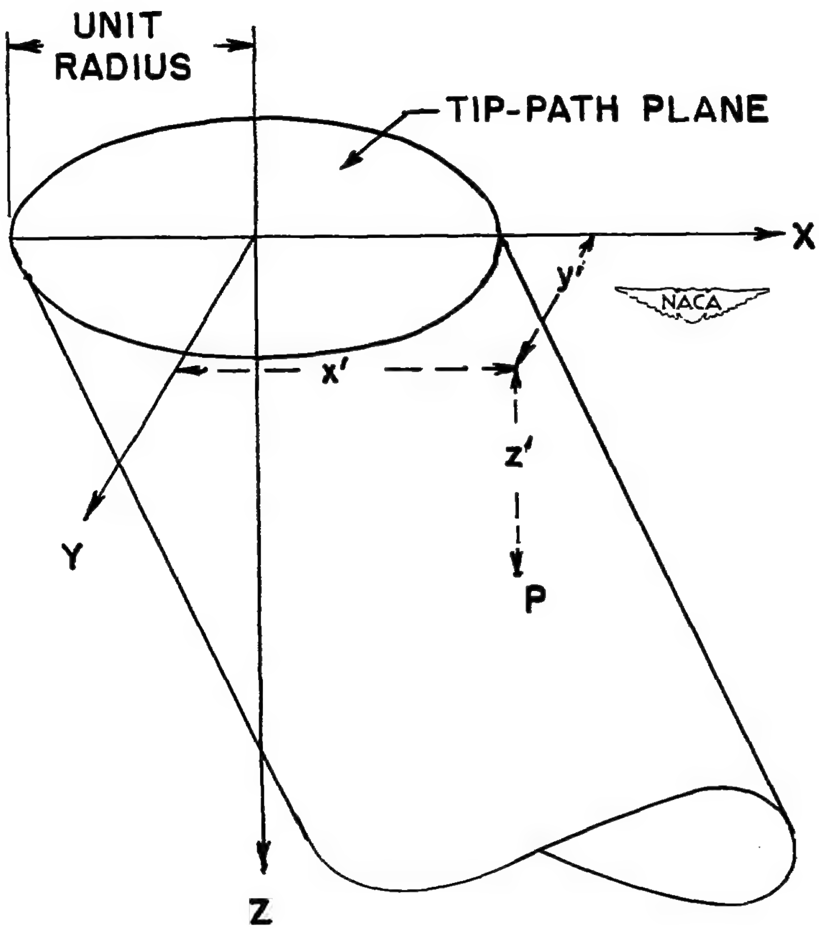

Figure 3.- Nondimensional rotor coordinates.

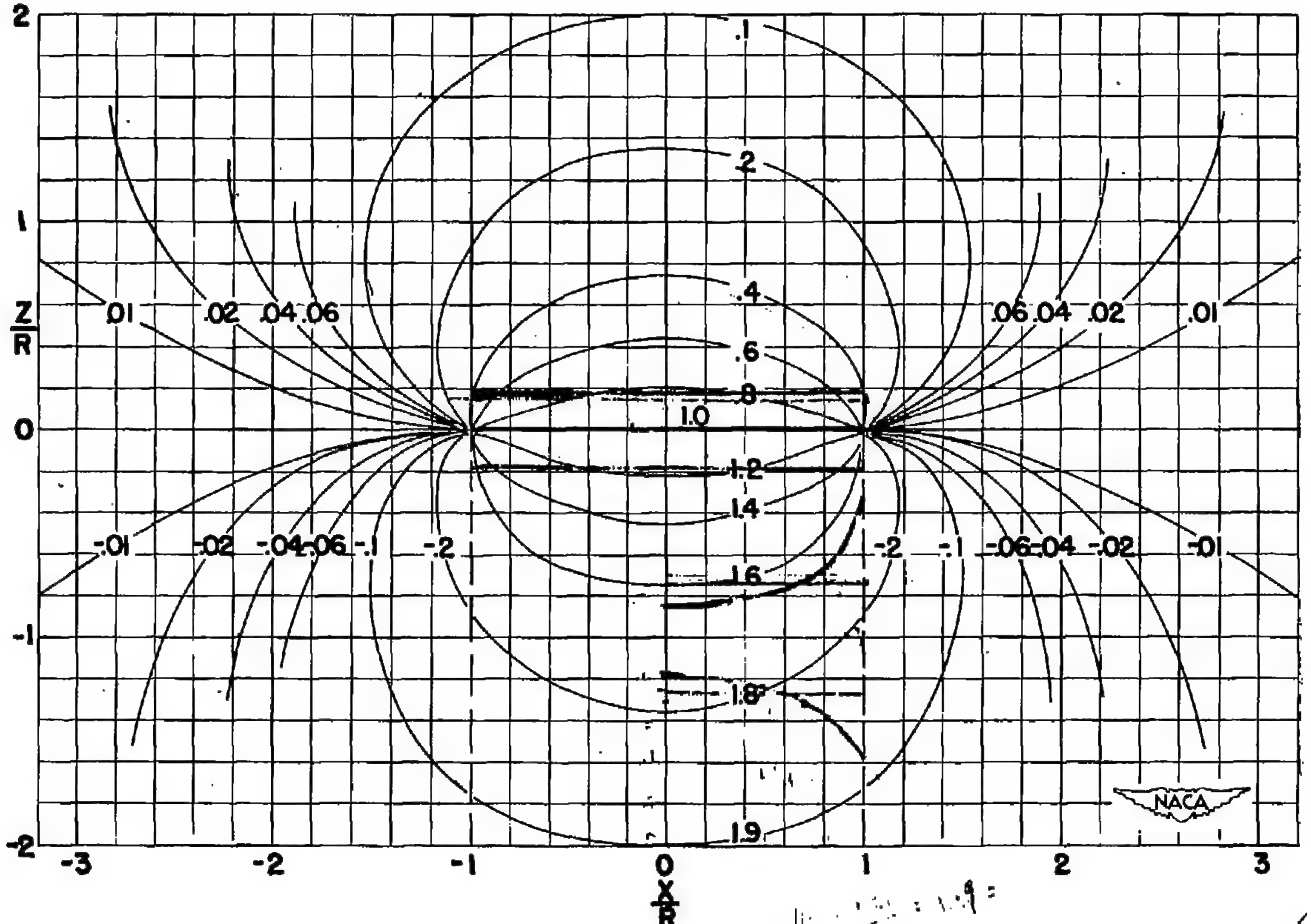

(a) $\chi = 0^{o} = \tan^{-1} 0$.

Figure 4.- Lines of constant values of isoinduced velocity ratio V_i/v in longitudinal plane of symmetry.

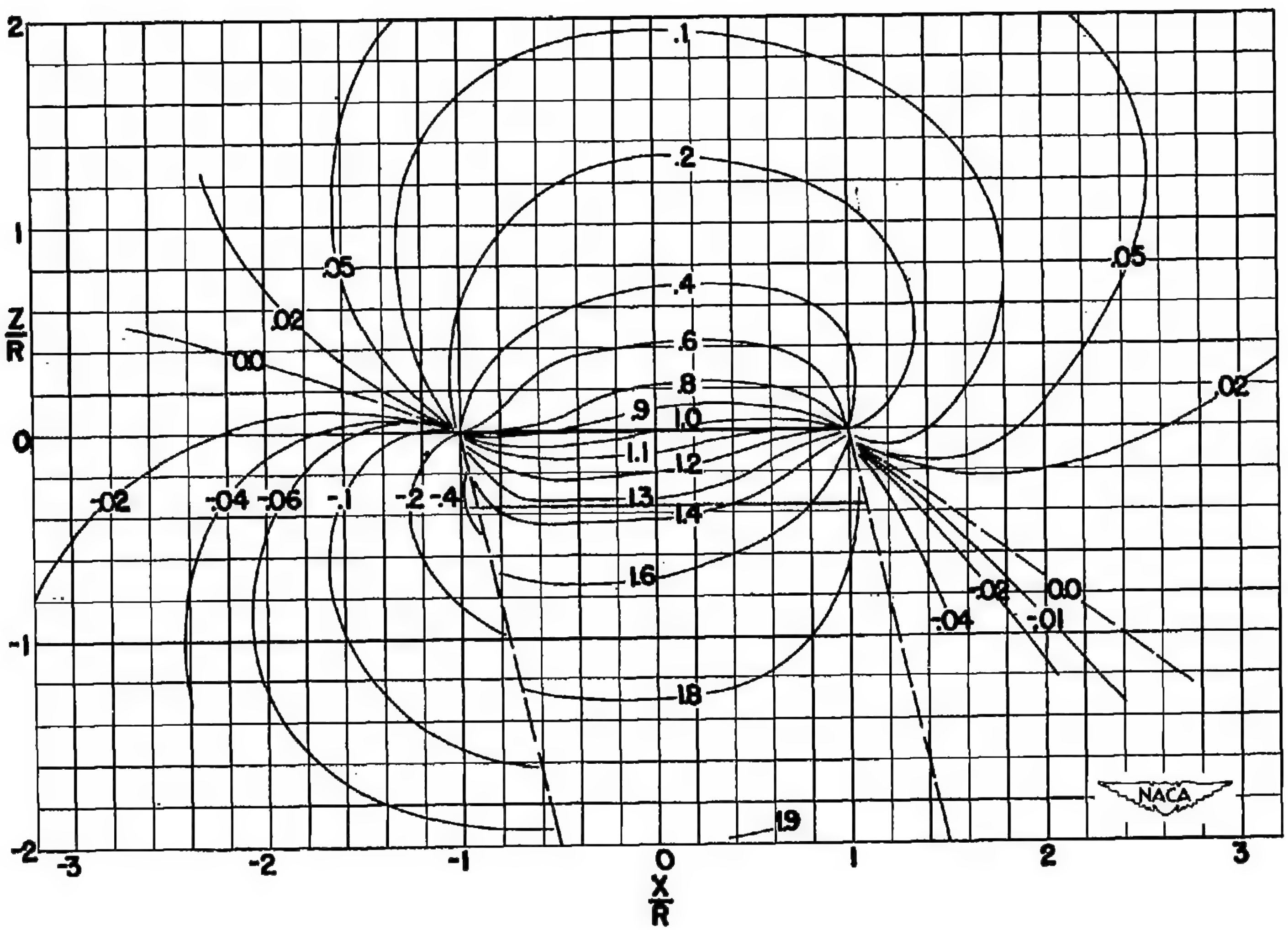

(b) $\chi = 14.04^{\circ} = \tan^{-1} 1/4$.

Figure 4.- Continued.

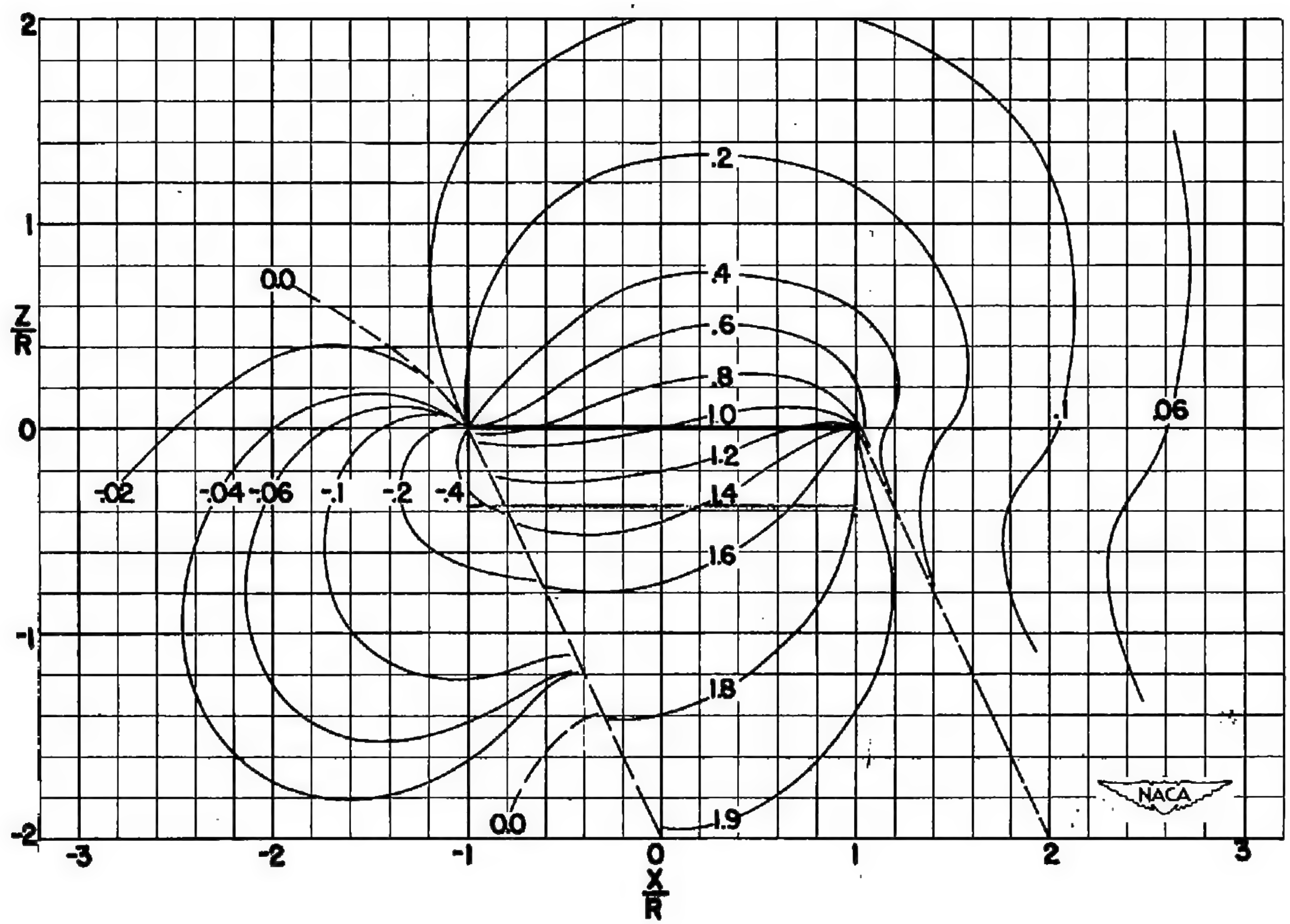

(c) $\chi' = 26.56^{\circ} = \tan^{-1} 1/2$.

Figure 4.- Continued.

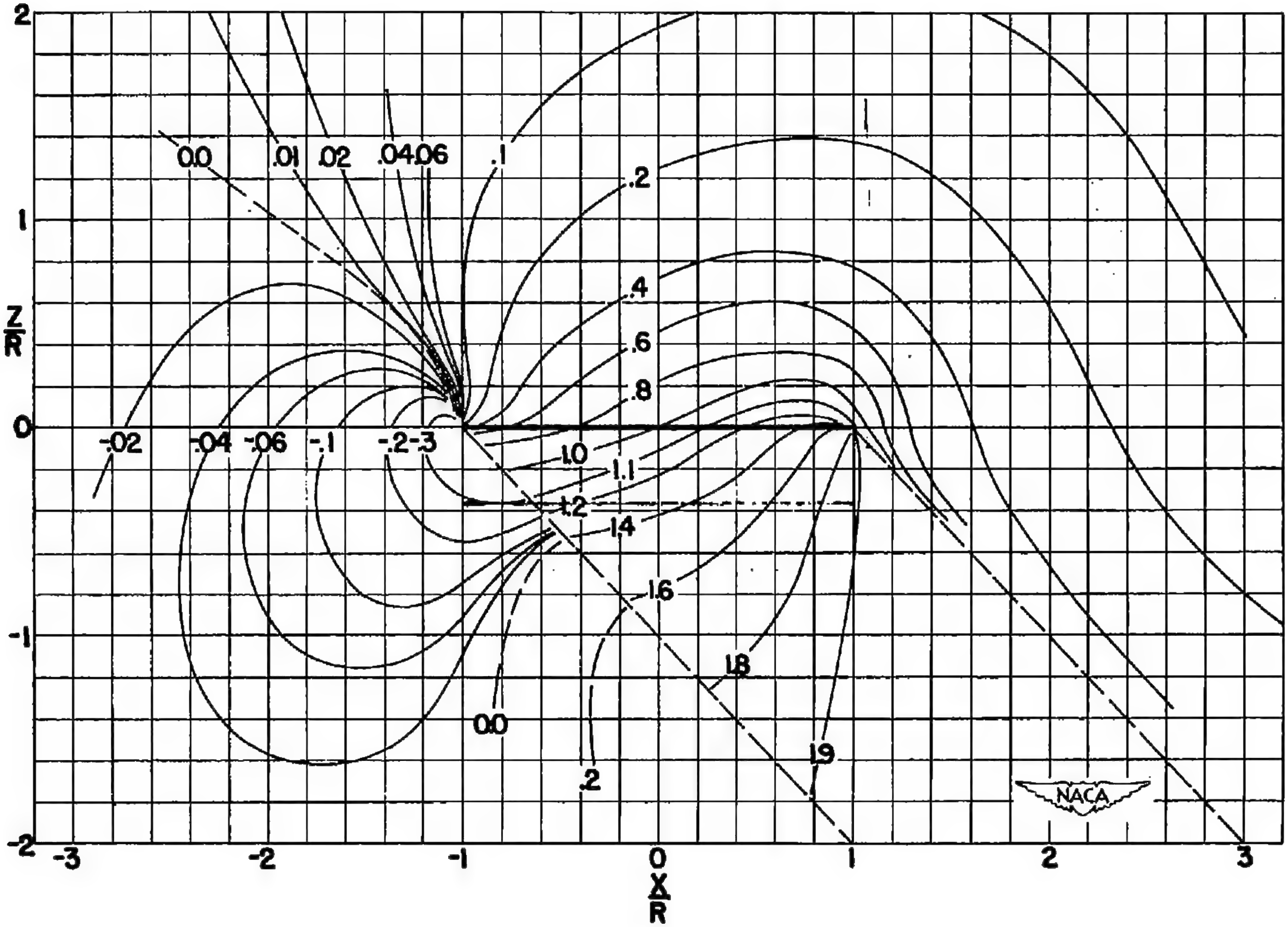

(d) $\chi = 45.00^{\circ} = \tan^{-1} 1$.

Figure 4.- Continued.

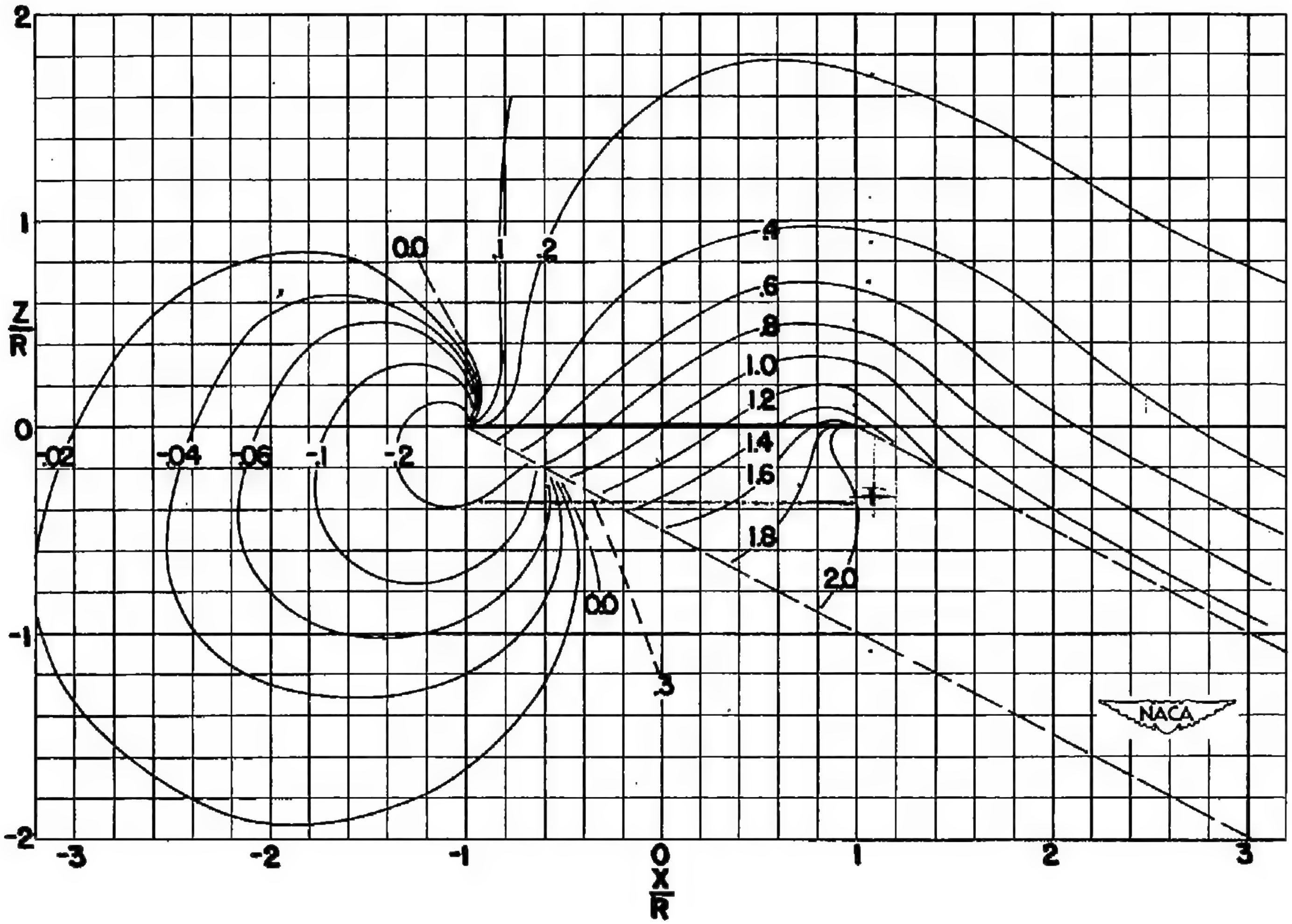

(e) $\chi = 63.43^{\circ} = \tan^{-1} 2$.

Figure 4.- Continued.

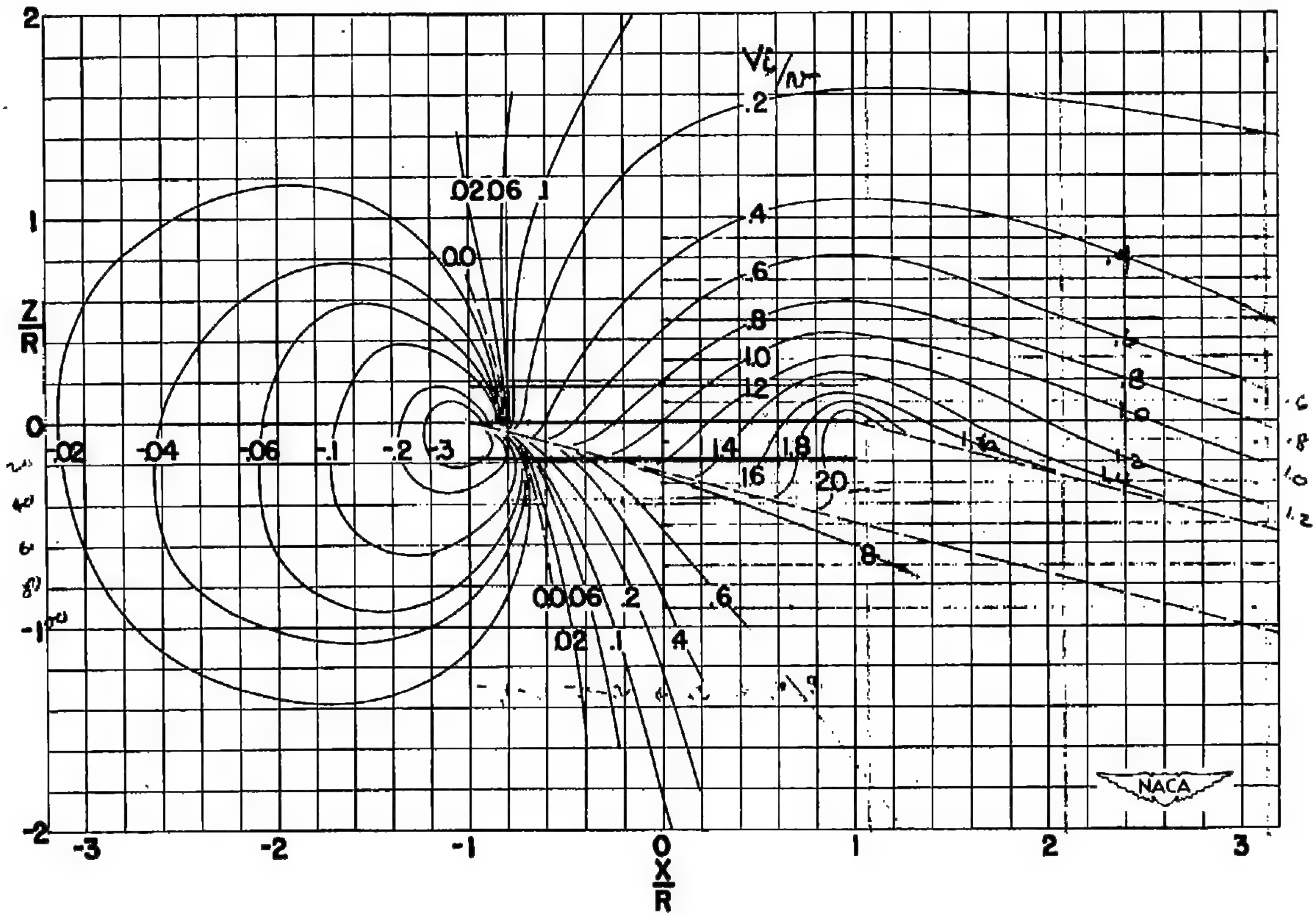

(f) $\chi = 75.97^{\circ} = \tan^{-1} 4$.

Figure 4.- Continued.

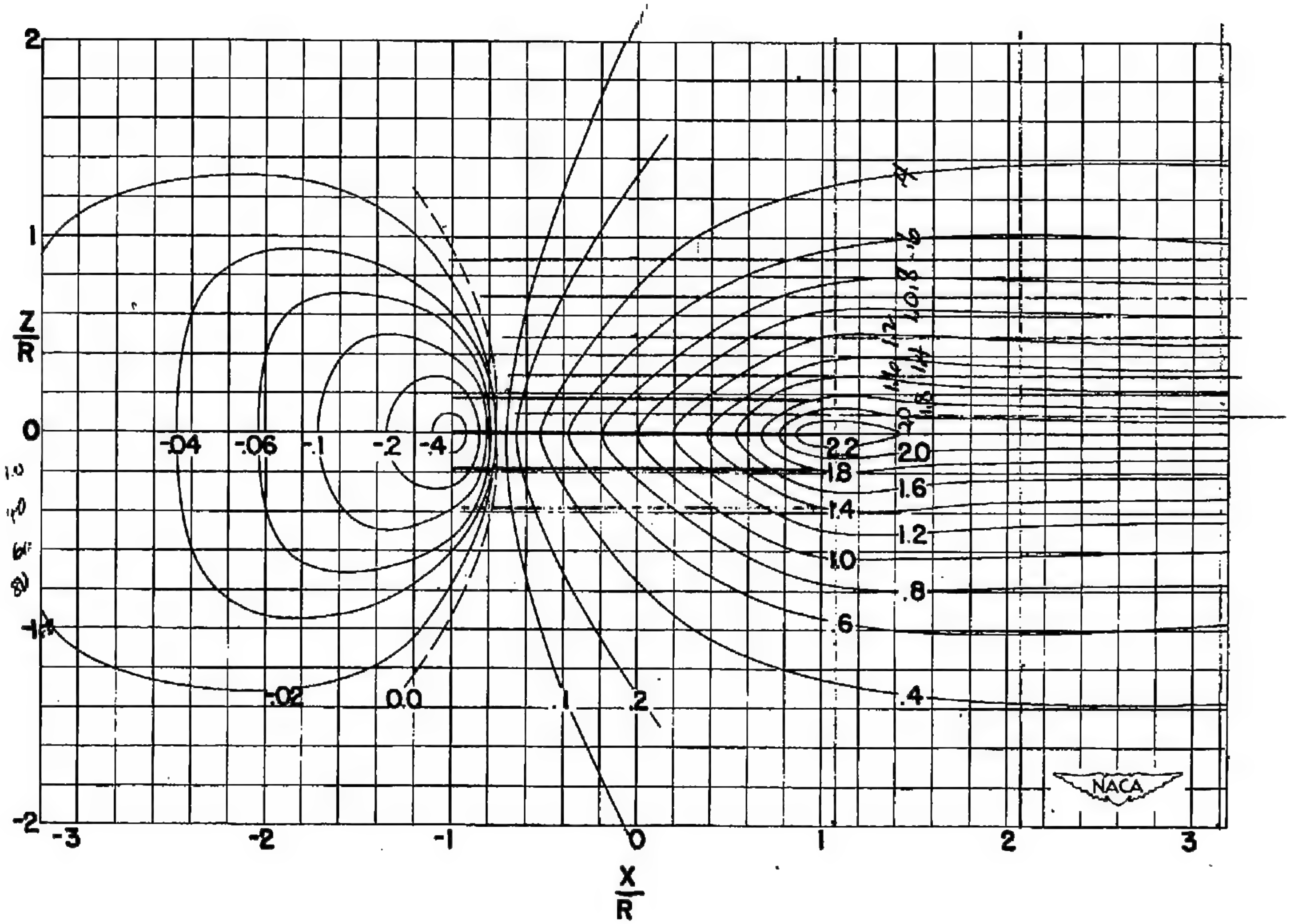

(g) $\chi = 90.00^{\circ} = \tan^{-1} \infty$.

Figure 4.- Continued.

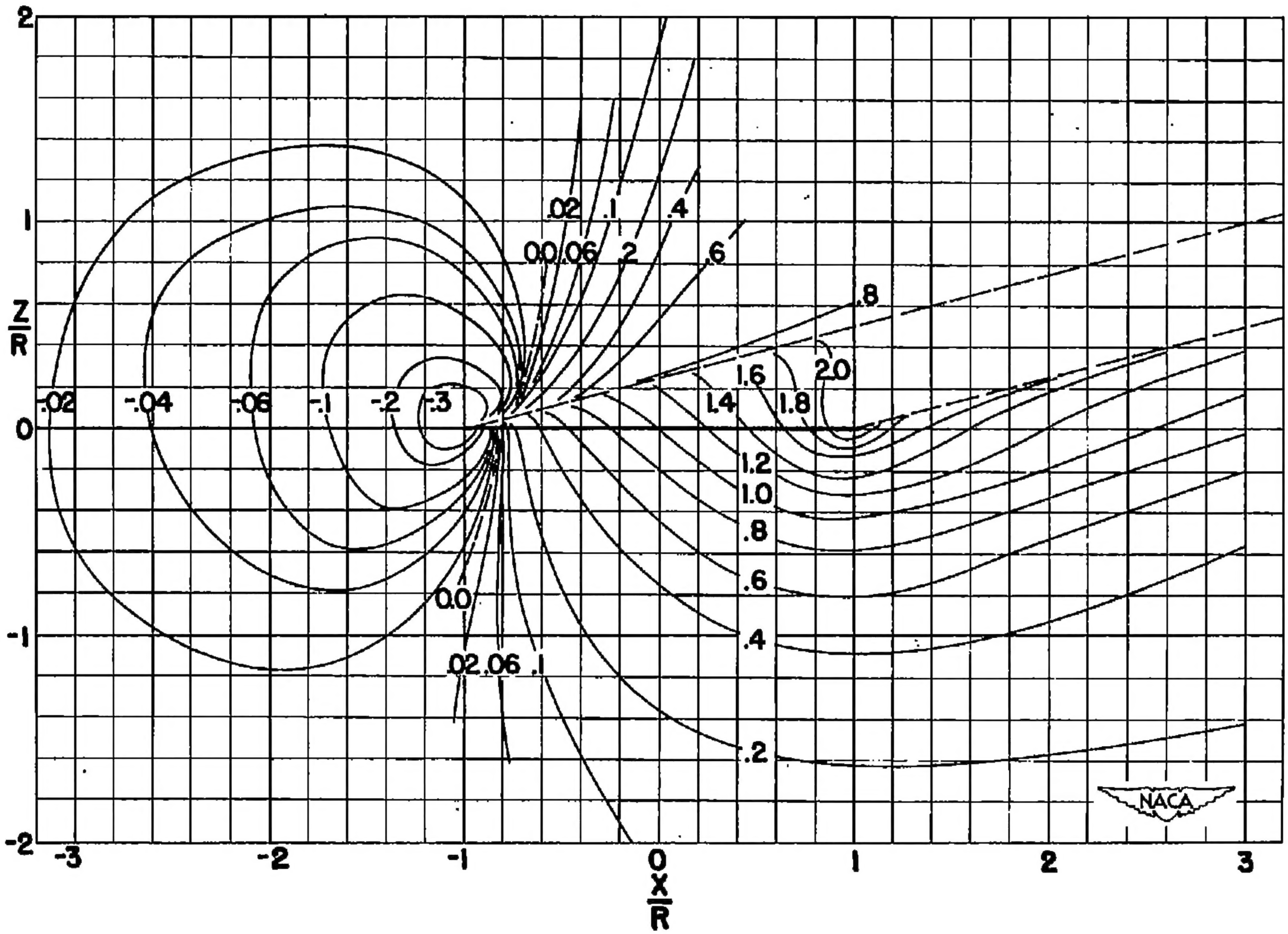

(h) $\chi = 104.03^{\circ} = \tan^{-1} -4$.

Figure 4.- Continued.

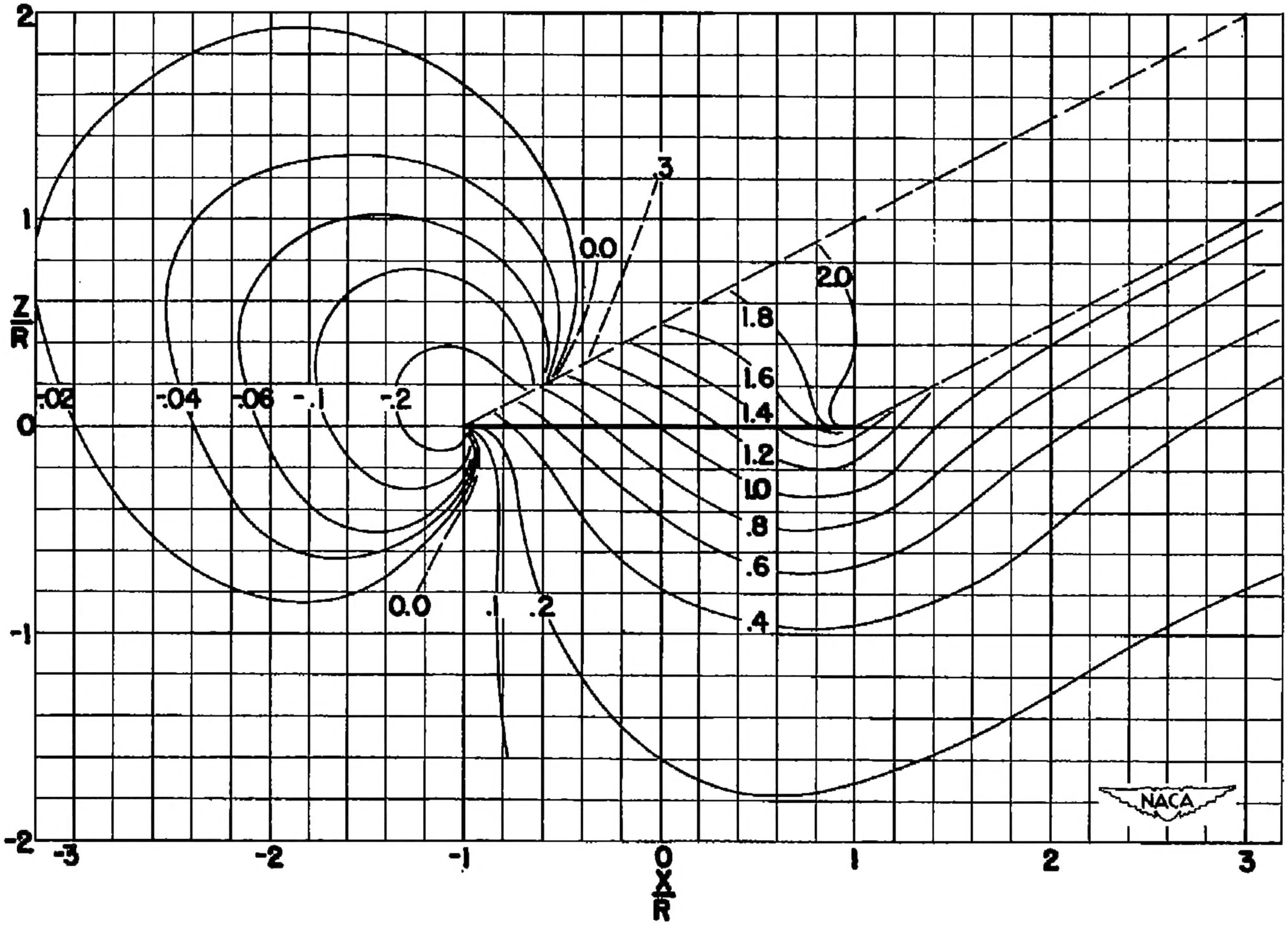

(i) $\chi = 116.57^{\circ} = \tan^{-1} -2$.

Figure 4.- Concluded.

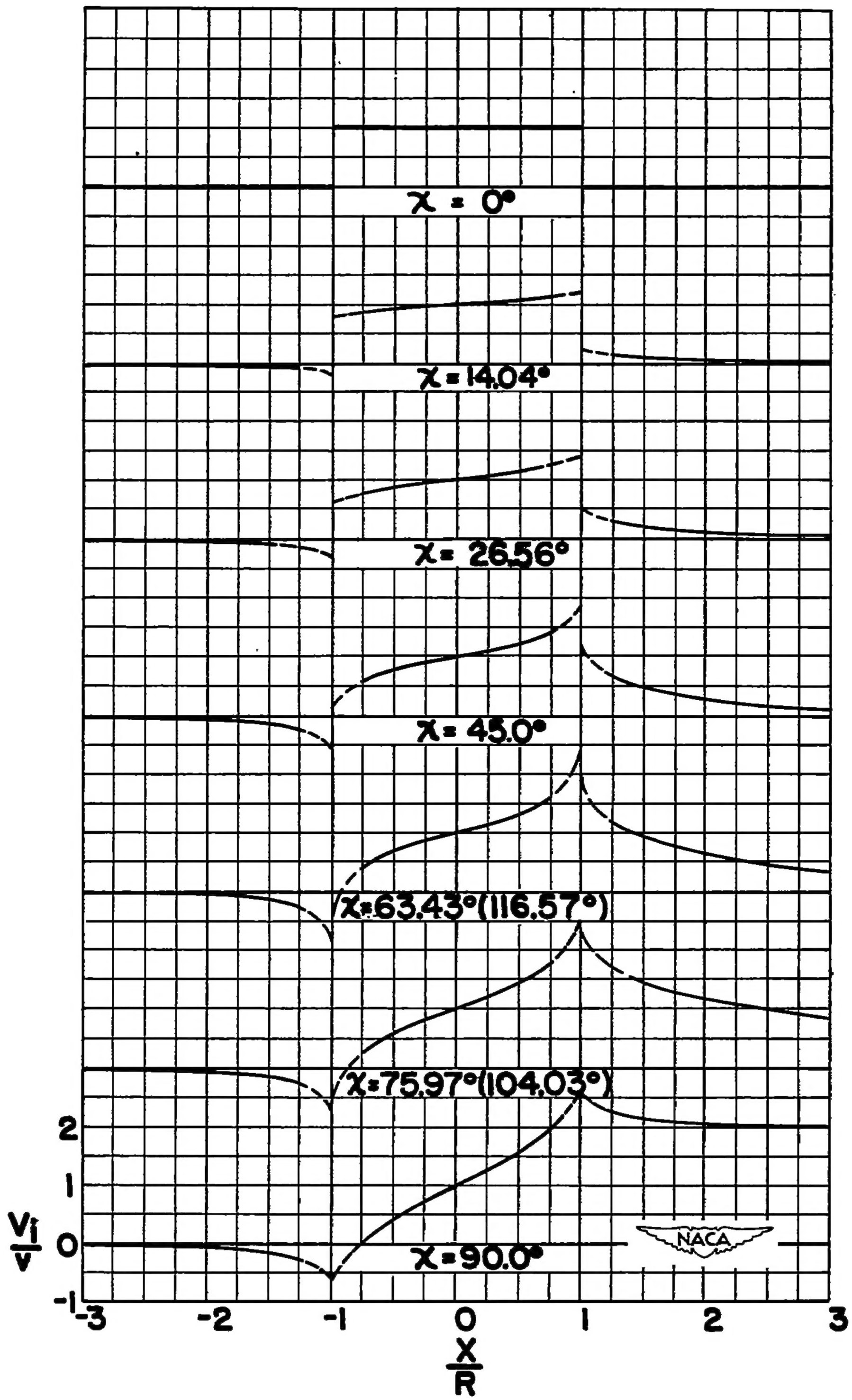

Figure 5.- Induced velocity distributions along X-axis.

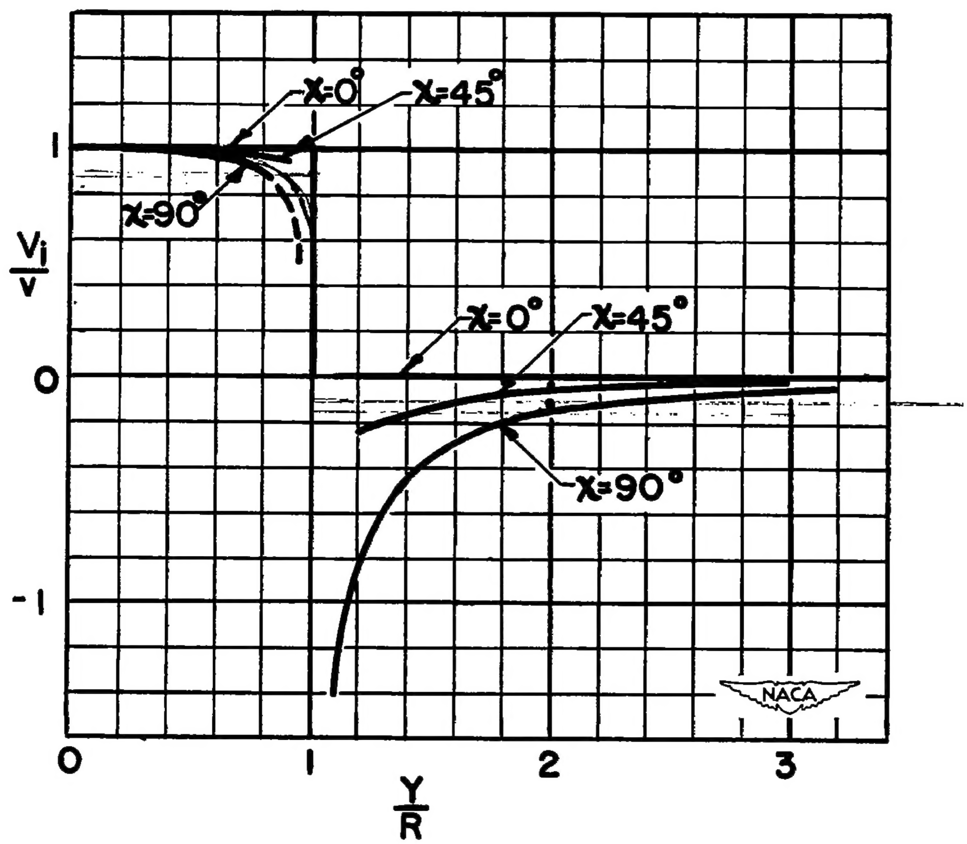

Figure 6.- Induced velocity distributions along Y-axis.

NACA-Langley - 3-20-53 -1000